

Learning with Wasserstein Barycenters and Applications

Research Article

G. N. Domazakis^{a,d}, D. Drivaliaris^e, S. Koukoulas^f, G. I. Papayiannis^{*a,c}, A. E. Tsekrekos^b, and A. N. Yannacopoulos^a

^aAthens University of Economics & Business, Department of Statistics, Stochastic Modeling and Applications Laboratory, Athens, GR

^bAthens University of Economics & Business, Department of Accounting and Finance, Athens, GR

^cHellenic Naval Academy, Section of Mathematics, Mathematical Modeling and Applications Laboratory, Piraeus, GR

^dUniversity of Sussex, Department of Mathematics, Brighton, UK

^eUniversity of the Aegean, Department of Financial and Management Engineering, Chios, GR

^fUniversity of the Aegean, Department of Geography, Mytilene, GR

Abstract

In this work, learning schemes for measure-valued data are proposed, i.e. data that their structure can be more efficiently represented as probability measures instead of points on \mathbb{R}^d , employing the concept of probability barycenters as defined with respect to the Wasserstein metric. Such type of learning approaches are highly appreciated in many fields where the observational/experimental error is significant (e.g. astronomy, biology, remote sensing, etc.) or the data nature is more complex and the traditional learning algorithms are not applicable or effective to treat them (e.g. network data, interval data, high frequency records, matrix data, etc.). Under this perspective, each observation is identified by an appropriate probability measure and the proposed statistical learning schemes rely on discrimination criteria that utilize the geometric structure of the space of probability measures through core techniques from the optimal transport theory. The discussed approaches are implemented in two real world applications: (a) clustering eurozone countries according to their observed government bond yield curves and (b) classifying the areas of a satellite image to certain land uses categories which is a standard task in remote sensing. In both case studies the results are particularly interesting and meaningful while the accuracy obtained is high.

Keywords: clustering; classification; geodesics; Wasserstein barycenter; remote sensing; yield curves;

1 Introduction

The majority of statistical learning methods refer to data which are considered as points on some high-dimensional Euclidean space (\mathbb{R}^d), and treat the problem of clustering them into like classes depending on their distance or similarity occurring from their location on the underlying space. Such methods have led to the development of powerful algorithms, as for example the K-means algorithm, which are widely used in statistical learning [15, 28]. On the other hand, the implementation of these algorithms has highlighted the importance of geometrical features such as dimension or the notion of distance employed in the underlying space on the results of the clustering process ([2, 7, 9]).

*Corresponding author: Patission Str. 76, Athens, 10434, Greece. E-mail: gpapayiannis@aueb.gr

However, in the new era of data science, the nature of data structures has significantly been enriched and evolved so that in many cases data can no longer be sufficiently represented as elements of some high dimensional Euclidean space \mathbb{R}^d . As a result, traditional methods in statistical learning may not be appropriate for analysing such types of complex data. Examples of such cases can be functional data [8, 17, 25], data sampled at high frequency [13, 20], interval data [10, 11, 16], spatial data [14], uncertain data [1], matrix-valued data [27], etc.

In this paper, we propose a framework under which complex data, which may not sufficiently be represented as vectors in \mathbb{R}^d , can be treated as elements of some space of probability measures, which when endowed with an appropriate metric structure, the Wasserstein metric, can lead to a better representation of such complex data. After recognizing the appropriate underlying space for the data, we develop a clustering and classification scheme in Wasserstein space, based on its geometry and concept of barycenter in order to characterize the cluster centers as well as the concept of geodesic to quantify similarity of observations within a particular cluster. Moreover, indices that (a) quantify the homogeneity of the induced clusters and (b) reveal the appropriate selection for the number of clusters are developed relying on geometric arguments on the space of probability measures. The proposed method is applied to two illustrative examples, (a) in quantitative finance and in particular the classification of sovereign bonds within credit classes, and (b) in remote sensing and in particular in the classification of pixels from satellite images into certain category types related to land uses.

2 Clustering in the Wasserstein space

In this section, we investigate clustering techniques that can be used for learning purposes in the space of probability measures (Wasserstein space) with the learning procedure being either supervised or unsupervised depending on the application. In particular, an extension of the well known K-means algorithm within the framework of probability measures is considered. We start by presenting some motivation from certain classes of complex data, which are more suitably treated as measure valued data, and introduce the problem of clustering such observations in the space of probability measures. Then, the extension of the original K-means algorithm to the probabilistic setting is discussed, i.e. the case where the observations to be clustered are probability distributions adopting the metric framework of Wasserstein spaces, in order to replace the usual Euclidean framework commonly employed in clustering studies. Employing the geometry of Wasserstein space, and in particular its geodesic structure, we propose a clustering criterion which quantifies the compactness of clusters and assists in the choice of the number of clusters.

2.1 Motivation and general framework

Consider a collection of data points x_1, x_2, \dots, x_n on \mathbb{R}^d , corresponding to some type of measurements. The standard clustering procedure would involve the application of a clustering algorithm, e.g. the K-means algorithm, considering these observations as points on the Euclidean space \mathbb{R}^d , endowed with the standard Euclidean metric, and the observations will be clustered according to their distance from fictitious centers located at certain positions in \mathbb{R}^d , in terms of the Euclidean distance. Such clustering procedures have been proved very successful in understanding the structure of data in statistical learning procedures. Even in the case where the data can be efficiently represented as elements of \mathbb{R}^d , the choice of metric with which this space is endowed may affect the clustering result (see e.g. [24]).

However, there are many instances where the data under consideration cannot naturally be represented on a linear space, either because of special constraints or because of their collection type and sampling method. In such cases the K-means algorithm has to be modified in order to take into account the non-linearity of the underlying space.

A large class of data types such as the ones described above, can be understood as measures and will henceforth be referred to as *measure-valued data*. In order to motivate this statement, we present below four particular examples.

Example 2.1 (Data that can be understood as probability measures). In many cases, we can assume that what we actually need from our observations, is not the value of the observation as such, but the collective behaviour of relevant data. For example, one may wish to consider the distribution of a physical quantity (e.g. temperature, wind speed) for a certain time period and wish to understand the differences between the distributions of the same quantity on different time periods or locations. Under this perspective, the individual data related to the particular time periods or locations will be used to obtain (empirical) estimations of the probability measures describing the quantity. Wishing to study the aggregate characteristics, which are described by the aforementioned probability measure, one may consider as observed data the induced probability measures, therefore leading to the framework of measure-valued data. Issues such as clustering or classification of these probability measures arise naturally. In fact some of the applications presented in paper can be understood as clustering measure-valued data, as for example the application in remote sensing in Section 3.2.

Example 2.2 (Data point clouds). Often, spatial data can be understood as data point clouds that carry some heterogeneity. A particular example can be the onset and evolution of an epidemic, in which the spatial location and severity of several incidents is of interest. Certain spatial locations may be hit with different severity and to classify such regions into clusters and assess the spatio-temporal allocation of risk. Data point clouds can be identified as empirical probability measures using convex combination of Dirac measures of the incidents taking into account location, frequency and severity or smoothed representations using appropriate kernel-based estimators.

Example 2.3 (Matrix-valued data). Other types of data can be perceived as measure-valued data, hence making feasible their treatment as elements of a Wasserstein space. An example of particular interest are matrix valued data and in particular correlation or covariance matrix data. As well known Gaussian measures on \mathbb{R}^d are uniquely determined by their mean and their covariance matrix hence there is an one-to-one correspondence between the space of centered Gaussian measures and the manifold of positive-definite matrices (the natural space for covariance matrices) (see, e.g. [21, 31]). Hence, one can metrize the later using the Wasserstein metric in the space of Gaussian measures. This metric is usually called the Bures-Wasserstein metric ([6]) and can be calculated explicitly in terms of formula (1) with zero locations. As a result, the proposed algorithm in Section 2.2 can be directly implemented without any modifications for clustering matrix-valued data. In fact, some of the applications presented in paper can be understood as clustering matrix valued data, as for example the application on bond returns in Section 3.1.

Example 2.4 (Uncertain data). In many cases the observations of a dataset are not that certain due to the effect of experimental or observational error, noise to data, inconsistencies of the monitoring equipment, etc. The uncertainty of the measurements introduces some fuzziness as to the exact location of the points on the Euclidean space. One way to take into account this fuzziness is to substitute the data points with probability measures $\mu_1, \mu_2, \dots, \mu_n$, each one centered at its location vector $m_i = x_i \in \mathbb{R}^d$, with a covariance matrix $S_i \in \mathbb{R}_+^{d \times d}$, with $\mathbb{R}_+^{d \times d}$ denoting the set of symmetric and positive definite matrices of dimension d , modeling the uncertainty as to the exact location of the point. If geometric intuition is of any use, we are substituting each data point $x_i \in \mathbb{R}^d$, with an ellipsoid in \mathbb{R}^d , located at $m_i = x_i$, whose principal axes are indicated by the eigenvectors of the covariance matrix S_i , and we assign a probability that the actual measurement is located within this ellipsoid in terms of the probability measure μ_i . The different dispersion matrix S_i corresponding to the different probability

measures μ_i model the possible differential uncertainty assigned to each measurement. This is a very reasonable and plausible assumption. For example, each measurement may be obtained by a different source or a different measurement procedure, e.g. they may correspond to measurements of a quantity performed at different geographic locations, where remoteness introduces observational errors (one can easily consider applications in observational astronomy, meteorology, medical imaging, remote sensing, etc).

Motivated by the above examples we consider a collection of measures μ_i for $i = 1, 2, \dots, n$ that arose from an observation process or some statistical experiments. We will restrict our attentions to the case of the family of Location-Scale probability laws, and assume that each probability measure is sufficiently characterized by a location and dispersion pair, (m_i, S_i) . In particular, we will treat our observations as elements in the set of probability measures with finite moments of second order denoted by $\mathcal{P}_2(\mathbb{R}^d)$, endowed with the topology induced by the quadratic Wasserstein metric (see e.g. [26, 29]). This is a natural choice for metrizing the space of probability measures consistent with the weak-* topology, with the Wasserstein metric providing an appropriate notion of distance between two probability measures, taking efficiently into account the geometrical structure and non-linear nature of the underlying space.

We now proceed to the question of clustering these measure-valued observations. Since clustering requires a notion of distance which is appropriate for quantifying divergence between the objects under consideration, we propose the use of the Wasserstein metric space for this purpose. For example, this choice of metric space setting, can accommodate all the applications mentioned in Examples 2.1-2.4. For instance, concerning Example 2.4 our proposal properly takes into account the observational uncertainty (which may be of different degrees depending on the observation) of the original measurements and when combined with the K-means clustering algorithm is expected to lead to more robust results. Note that in the limit as $S_i \rightarrow 0$, the probability measure μ_i degenerates to Dirac mass δ_{x_i} on \mathbb{R}^d , and the Wasserstein distance $W_2(\mu_i, \mu_j)$ degenerates to the standard Euclidean distance $\|x_i - x_j\|_2$ in \mathbb{R}^d . Similar comments can be made also for the other examples.

We close the discussion by indicating why we expect that a K-means algorithm based on the Wasserstein distance to lead to different results. This is best illustrated, within an example in which in terms of a limiting procedure we may pass from a description of data in Euclidean space to its description in measure space; the example of uncertain data (Example 2.4) is ideally suited for this purpose. Consider that at some point in the course of the clustering procedure we have two potential cluster centers $\bar{x}_{c_1}, \bar{x}_{c_2} \in \mathbb{R}^d$ and an observation $y \in \mathbb{R}^d$ that has to be assigned to one of these two centers. Assume without loss of generality that $\|y - \bar{x}_{c_1}\|_2 < \|y - \bar{x}_{c_2}\|_2$ so that observation y is assigned to the cluster c_1 centered at \bar{x}_{c_1} . Consider now the case where observational uncertainty is assigned to the observations. Since the potential cluster centers are obtained dynamically as centroids of subsets of the original observations, the uncertainty concerning the observations propagates to some uncertainty as to the true location of the centers $\bar{x}_{c_1}, \bar{x}_{c_2}$. In the framework described above, this uncertainty is modeled by considering both the observation to be assigned to a particular cluster, as well as the centers of the two potential clusters the observations belongs to, as probability measures $\mu, \bar{\mu}_{c_1}, \bar{\mu}_{c_2} \in \mathcal{P}_2(\mathbb{R}^d)$, with locations and dispersions $(m, S) = (x, S)$, $(\bar{m}_1, \bar{S}_1) = (\bar{x}_{c_1}, \bar{S}_1)$, $(\bar{m}_2, \bar{S}_2) = (\bar{x}_{c_2}, \bar{S}_2)$, respectively, with the covariance matrices reflecting the extent and the nature of the observational uncertainty.

Let us assume that these probability measures belong to the same Location-Scatter family, say without loss of generality the Gaussian family, which is a good choice for modeling observational uncertainty on account of the central limit theorem. Taking this uncertainty into account we must necessarily use the Wasserstein distance between the resulting probability measures as a criterion of assigning the point $\mu \in \mathcal{P}_2(\mathbb{R}^d)$ to one of the two clusters centered at the points $\bar{\mu}_{c_1}, \bar{\mu}_{c_2} \in \mathcal{P}_2(\mathbb{R}^d)$. Using this criterion we will assign the point μ to the cluster $c \in \{c_1, c_2\}$ by setting $c = \arg \min_{c \in \{c_1, c_2\}} \{W_2(\mu, \bar{\mu}_{c_1}), W_2(\mu, \bar{\mu}_{c_2})\}$. According to [4] (please see Section 2.4),

we have that

$$(1) \quad W_2^2(\mu, \bar{\mu}_{c_j}) = \|m - \bar{m}_{c_j}\|_2^2 + Tr \left(S + \bar{S}_j - 2(S^{1/2}\bar{S}_jS^{1/2})^{1/2} \right), \quad j = 1, 2.$$

From this expression it becomes clear how uncertainty may alter the assignment to a particular cluster. Suppose that $\|m - \bar{m}_{c_1}\|_2 < \|m - \bar{m}_{c_2}\|_2$, so that the standard Euclidean K-means assigns this observation to cluster c_1 . If

$$Tr \left(S + \bar{S}_1 - 2(S^{1/2}\bar{S}_1S^{1/2})^{1/2} \right) > Tr \left(S + \bar{S}_2 - 2(S^{1/2}\bar{S}_2S^{1/2})^{1/2} \right),$$

then using the Wasserstein distance the same observation will be assigned to cluster c_2 instead. This difference in assignment is attributed as an effect of observational uncertainty and will lead to more robust clustering of the uncertain data. As a nice geometric intuitive approach consider ellipsoids of different orientations that have to be accommodated to different clusters. Clearly, the orientation of each ellipsoid plays a role as to which cluster it is appended to.

2.2 The Wasserstein K-means algorithm

Motivated by the discussion in the previous section we consider the following problem: Given a collection of measure valued data (which arise from complex data e.g. of the type mentioned in Examples 2.1-2.4) cluster the data into like groups. On account of the nonlinear nature of the space of probability measures (or probability distributions) the standard K-means algorithm in Euclidean space is no longer sufficient for this task. On the other hand, clustering is heavily based on the concept of distance between the objects which are to be separated, hence an appropriate metrization of the space of probability measures has to be adopted before we may proceed further to our goal. A very appropriate concept of distance for quantifying divergences between different probability measures is the Wasserstein distance which is compatible with the topology of the space of probability measures (see [26, 29] for justification of this metric properties). The Wasserstein distance is in general expressed as the standard optimal transport problem originated by [23]. Given a quadratic cost functional, for any two probability measures $\mu, \nu \in \mathcal{P}(\mathbb{R}^d)$ the Wasserstein distance is mathematically expressed as the minimization problem

$$(2) \quad W_2(\mu, \nu) = \inf_{T \in \mathcal{TM}(\nu)} \left\{ \int_{\mathbb{R}^d} \|x - T(x)\|^2 d\mu(x) \right\}^{1/2}$$

where $\mathcal{TM}(\nu) := \{T : \mathbb{R}^d \rightarrow \mathbb{R}^d : X \sim \mu, T(X) \sim \nu\}$ i.e. denotes the space of transport maps that *reshape* the random variable $X \in \mathbb{R}^d$ which is distributed according to the probability measure μ to the random variable $Y := T(X) \in \mathbb{R}^d$ distributed according to the probability measure ν . In other words, the optimal transport map T^* *pushes-forward* the measure μ to the measure ν , i.e. $\nu(A) = T^*\mu(A)$ for any Borel subset $A \subset \mathbb{R}^d$.

Assume that there is a collection of n probability measures $\mathcal{M} := \{\mu_1, \mu_2, \dots, \mu_n\}$ on \mathbb{R}^d . The problem under consideration is to separate this collection of measures into K clusters with the criterion of their “affinity” in the space of probability measures on \mathbb{R}^d ($\mathcal{P}(\mathbb{R}^d)$), requiring finite second moments, $\mathcal{P}_2(\mathbb{R}^d)$, endowed with the metric structure induced by the quadratic Wasserstein metric, $W_2(\cdot, \cdot)$. As the initial step of the clustering procedure, K points on $\mathcal{P}_2(\mathbb{R}^d)$ (probability measures) should be chosen as the initial cluster centers (this measures could be chosen either randomly or according to some rule, e.g. the most distant measures between them). Then, the cluster membership of each measure $\mu_i \in \mathcal{M}$ is determined according to the minimal Wasserstein distance criterion of this measure from each one of the centers (note that the minimal Wasserstein distance is equivalent to the minimal length curve connecting each point with each cluster center). Next, the cluster centers are updated according to the mean sense derived by the Wasserstein barycenter of the measures classified to each cluster, i.e. the notion of mean element in a set of probability measures employing the metric sense of

the Wasserstein distance. In particular, given that the measures $\mu_{k,i}$ for $i = 1, 2, \dots, n_k$ are the measures that have been assigned to the k -th cluster, the new k -th cluster center is determined through the solution of the minimization problem

$$(3) \quad \bar{\mu}_k = \arg \min_{\nu \in \mathcal{P}_2(\mathbb{R}^d)} \frac{1}{n_k} \sum_{i=1}^{n_k} \mathcal{W}_2^2(\nu, \mu_{k,i}),$$

i.e. through the determination of the Wasserstein barycenter (or just probability barycenter) of the measures that have been assigned to this particular cluster (later we will refer to this probability barycenter also as the k -th *local barycenter*). General existence, uniqueness and consistency results about Wasserstein barycenters for measures on \mathbb{R}^d have been established in [3, 18, 19]. The above steps of the clustering algorithm are repeated until no significant change on the cluster centers or their memberships occurs. The algorithm is presented briefly below (Algorithm 1).

Algorithm 1: Wasserstein K-Means

- 1 Choose K measures out of the original observations as the initial cluster centers, $\bar{\mu}_k$, $k = 1, \dots, K$.
- 2 At step m assign each of the measures μ_i , $i = 1, \dots, n$, to one of the K clusters, choosing the cluster membership $k(i)$ according to the rule

$$k(i) = \arg \min_{k \in \{1, 2, \dots, K\}} \mathcal{W}_2^2(\mu_i, \bar{\mu}_k^{(m)}).$$

- 3 Update the cluster centers $\{\bar{\mu}_k^{(m)}\}_{k=1}^K$, through the rule

$$\bar{\mu}_k^{(m)} := \arg \min_{\nu \in \mathcal{P}_2(\mathbb{R}^d)} \frac{1}{n_k} \sum_{i=1}^{n_k} \mathcal{W}_2^2(\nu, \mu_{k,i}^{(m)}), \quad \text{for all } k = 1, 2, \dots, K,$$

where $\mu_{k,i}^{(m)}$ denotes the i -th measure of the n_k that have been assigned to the k -th cluster at step m .

- 4 Repeat steps 2-3 until the cluster centers do not change significantly.

2.3 The geometric interpretation of the clustering procedure

In this subsection, we discuss the geometric interpretations that can be extracted by the clustering procedure of the Wasserstein K-Means algorithm (Algorithm 1). Following the previous discussion, each one of the K cluster centers under the proposed setting coincides with the Wasserstein barycenter of all the measures that belong to that cluster. Denote by $\bar{\mu}_k$ for $k = 1, 2, \dots, K$ the cluster centers or *local barycenters* and as $\bar{\mu}_0$ the barycenter of all measures or the *global barycenter*. Since all the measures involved belong to the same space we are able to define the *shortest paths* that connect these points, i.e. their *geodesic curves*. A very interesting characterization of these curves is provided by [22] called the McCann's interpolant and relies on the concept of optimal transport maps.

According to McCann, the geodesic curve (or shortest path) that connects two measures μ, ν in Wasserstein space can be formulated as the set of parameterized curves

$$(4) \quad \gamma(t) = \{[(1-t)I + tT]_{\#}\mu\}_t, \quad t \in [0, 1],$$

where $\gamma(0) = \mu$ and $\gamma(1) = \nu$, T is the optimal transport map that pushes-forward the measure μ to the measure ν and I denotes the identity operator, i.e. $I_{\#}\mu = \mu$. According to this

construction, the minimum length connections between the global barycenter $\bar{\mu}_0$ and the local barycenters $\bar{\mu}_k$ for $k = 1, \dots, K$ are characterized by the parameterized curves

$$(5) \quad \gamma_k(t) = \{[(1-t)I + tT^{(k)}]_{\#}\bar{\mu}_0\}_t, \quad t \in [0, 1], \quad k = 1, \dots, K$$

where $T^{(k)}$ denotes the optimal transport map that pushes forward the global barycenter to the k -th local barycenter, i.e. $T_{\#}^{(k)}\bar{\mu}_0 = \bar{\mu}_k$ and it holds that $\gamma_k(0) = \bar{\mu}_0$ and $\gamma_k(1) = \bar{\mu}_k$. Using these shortest path connections between the local barycenters and the global barycenter we try to characterize the cluster membership of the probability measures involved in the clustering task which will lead to a compactness index for the shaped clusters.

Let μ_i be an arbitrary measure that needs to be assigned to one of the K clusters. It is clear from the K-means algorithm that the cluster where the measure μ_i will be assigned to, is the cluster which center $\bar{\mu}_k$ will have the minimal (Wasserstein) distance from μ_i , or in other words, the geodesic curve that connects the measure μ_i with the specified local barycenter $\bar{\mu}_k$ must have the smallest length comparing to the lengths of each one of the other geodesic curves $\{\gamma_k(\cdot)\}$ for all $k = 1, 2, \dots, K$. Since the measure μ_i is assigned to the k -th cluster, then the k -th geodesic curve connecting the global barycenter $\bar{\mu}_0$ with the k -th local barycenter $\bar{\mu}_k$ may reveal more information regarding this assignment. This extra information is revealed by the point on the geodesic $\gamma_k(t)$ that the measure μ_i is closest, i.e. the projection of measure μ_i to the geodesic curve $\gamma_k(t)$ (projection in terms of the Wasserstein distance). The closest point location alongside this particular geodesic curve is represented by $\tau_i \in [0, 1]$, called the *registration parameter*, and its value is obtained through the solution of the optimization problem (*registration problem*)

$$(6) \quad \tau_i := \arg \min_{t \in [0, 1]} W_2^2(\mu_i, \gamma_k(t)).$$

The registration of measure μ_i to the geodesic curve γ_k , can be considered as some sort of interpolation scheme, which allows us to approximate this measure by a measure considered as an interpolant between the global barycenter (i.e. mean of all observations) $\bar{\mu}_0$ and the barycenter of the particular cluster to which the particular observation (measure μ_i) is assigned to by the K-means algorithm. The registration parameter τ_i is a similarity index, indicating whether the derived approximation is closer to the general global barycenter $\bar{\mu}_0$ or the barycenter $\bar{\mu}_k$ of the k cluster. In particular $\tau_i = 1$ indicates coincidence of μ_i with the cluster center and $\tau_i = 0$ indicates coincidence with the global barycenter. As a result of that, the value of the parameter τ_i can be conceived as a quantification of the membership of the projection of μ_i to the particular cluster k it is assigned to. The membership is stronger the closer τ_i is to 1.

The later interpretations are not completely true since the measure μ_i will not coincide with any other measure unless their distance is zero. Therefore, the value τ_i itself may provide a first sense of similarity of the particular measure with the cluster center, however without taking into account also the distance between them, any conclusion could be proved misleading. Therefore, instead of using only the value τ_i to quantify the similarity of the measure μ_i to the k -th local barycenter, we should take also into account the distance of measure μ_i from the cluster center, i.e. $\sigma_i := W_2(\mu_i, \bar{\mu}_k)$, or the distance from the point's projection on the geodesic curve, i.e. $\tilde{\sigma}_i := W_2(\mu_i, \gamma_k(\tau_i))$ (see Figure 1). Clearly, the pair (τ_i, σ_i) or the pair $(\tau_i, \tilde{\sigma}_i)$ provide valuable information regarding the *goodness of fit* of μ_i to the k -th cluster and its contribution to the cluster's variability. On Section 2.5 we construct a cluster compactness index based on the information provided by these pairs.

Note that these pairs can enhance with a fuzzy character the whole clustering procedure. For example, assigning μ_i to a specific cluster which registration parameter τ_i has value close to 0, can have the interpretation that the cluster center is closer to this specific observation but the cluster membership is extremely ambiguous since the two measures are not that similar. On the other hand, an assignment to a cluster accompanied by a registration parameter value close

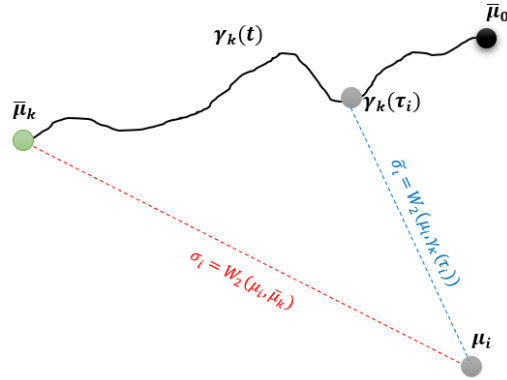


Figure 1: *Cluster membership characterization of a point $\mu_i \in \mathcal{P}(\mathbb{R}^d)$ using its projections to the local geodesic curve connecting the global barycenter ($\mu_0 \in \mathcal{P}(\mathbb{R}^d)$) with the local barycenters that $\bar{\mu}_k$ deviates less.*

to 1 means that the cluster membership looks a very natural choice. However, in the second case the value of σ_i or $\tilde{\sigma}_i$ may chance entirely the conclusion if its value is too big (we discuss this matter later on Section 2.5).

2.4 The proposed clustering procedure for the case of Gaussian measures

In this section we discuss the special but very common in practice case where the probability measures involved are members of the Location-Scatter family. In the proposed clustering approach, this particular parametric family is of great interest since the afore mentioned results can be expressed in explicit or semi-explicit form. First, we summarize the results of [4] regarding the Wasserstein distance between two probability measures on \mathbb{R}^d belonging to the same Location-Scatter family as well as an efficient scheme for the calculation of the Wasserstein barycenter for a collection of probability measures from distributions of this type.

In general, a Location-Scatter family is a family of probability laws on \mathbb{R}^d , induced by positive definite and affine transformations of the form $AX + m$, where $A \in \mathcal{M}_+^{d \times d}$ ($\mathcal{M}_+^{d \times d}$ denotes the set of positive definite and symmetric matrices with d diagonal elements), $m \in \mathbb{R}^d$ and X is a random vector in \mathbb{R}^d following the probability law $\mu_0 \in \mathcal{P}_{2,ac}(\mathbb{R}^d)$ (the set of probability measures on \mathbb{R}^d with finite second-order moments and absolutely continuous with respect to the Lebesgue measure). This family is denoted by $\mathcal{LS}(\mu_0) := \{\mathcal{L}(AX + m), A \in \mathcal{M}_+^{d \times d}, m \in \mathbb{R}^d, \mu_0 = \mathcal{L}(X)\}$. An alternative parametrization of a location-scatter family can also be obtained in terms of the location vector m_0 and the dispersion matrix S_0 of the defining measure μ_0 , in terms of $\mu_0^* := \mathcal{L}(S_0^{-1/2}(X_0 - m_0))$. Location-Scatter families constitute a large class of probability laws in \mathbb{R}^d including important cases such as the Gaussian family. The quadratic Wasserstein distance of two probability measures of the same Location-Scatter family μ_1, μ_2 , each characterized in terms of the location vectors and covariance-matrices $(m_1, S_1), (m_2, S_2)$, is given explicitly in terms of the expression

$$(7) \quad \mathcal{W}_2^2(\mu_1, \mu_2) = \|m_1 - m_2\|_2^2 + \text{Tr} \left(S_1 + S_2 - 2(S_1^{1/2} S_2 S_1^{1/2})^{1/2} \right)$$

Importantly, this exact result is also a lower bound for the Wasserstein distance of any pair of probability measures μ_1, μ_2 , with locations and covariances $(m_1, S_1), (m_2, S_2)$, **not** necessarily belonging to the same family of location-scatter families.

We also remind that given a collection of probability measures $\{\mu_i\}_{i=1,\dots,n}$ and a weight vector $w = (w_1, \dots, w_n) \in \Delta^n$ belonging to the unit simplex, the Wasserstein barycenter of the

collection for the given set of weights is defined as the minimizer of the problem:

$$\mu_B(w) := \arg \min_{\mu \in \mathcal{P}_2(\mathbb{R}^d)} \sum_{i=1}^n w_i \mathcal{W}_2^2(\mu, \mu_i).$$

General conditions on the existence of the Wasserstein barycenter have been given by [3], who also studied the special case of Gaussian measures, while an alternative approach to this problem in terms of a fixed point characterization has been proposed in [4]. In both these references it has been shown independently that when the collection of measures $\{\mu_i\}_{i=1,\dots,n}$ comes from the same Location-Scatter family, the measure $\mu_B(w)$ (i.e. barycenter) is a measure from the same family with location and dispersion parameters determined by the pair (m_B, S_B) , where m_B can be explicitly expressed as

$$(8) \quad m_B = \sum_{i=1}^n w_i m_i,$$

and S_B is the unique solution to the matrix equation

$$(9) \quad S_B = \sum_{i=1}^n w_i \left(S_B^{1/2} S_i S_B^{1/2} \right)^{1/2}.$$

An iterative fixed point algorithm for the approximation of the solution of the above matrix equation has been proposed in [4] where the solution S_B is approximated through the iteration scheme

$$M_{k+1} = M_k^{-1/2} \left(\sum_{i=1}^n w_i (M_k^{1/2} S_i M_k^{1/2})^{1/2} \right)^2 M_k^{-1/2}, \quad n \geq 0,$$

for some initial condition $M_0 \in \mathbb{R}_+^{d \times d}$.

Following the aforementioned explicit form results for the Wasserstein distance and Wasserstein barycenter in the case of Location-Scatter family, we can obtain also analytic expressions for the optimal transport maps and very convenient properties for the geodesic curves between such type of measures. Since the case of Gaussian measures is applied widely in multivariate statistics we focus on this case. Consider the Gaussian measures $\mu_0, \mu_1 \in \mathcal{P}(\mathbb{R}^d)$ with location parameters $m_0, m_1 \in \mathbb{R}^d$ and dispersion matrices $S_0, S_1 \in \mathbb{R}_+^{d \times d}$ respectively. Due to the regularity of these measures, there exists a unique optimal transport map T that pushes forward measure μ_0 to μ_1 , i.e. $T_{\#} \mu_0 = \mu_1$. In the case of Gaussian measures of the same location (consider $m_0 = m_1 = \mathbf{0}$), this mapping is the symmetric and positive definite matrix $\Lambda = S_1^{1/2} (S_1^{1/2} S_0 S_1^{1/2})^{-1/2} S_1^{1/2}$ (please see [22]). Therefore if a random variable X is distributed according to the law $N(\mathbf{0}, S_0)$, then its transformation $Y := \Lambda X$ is distributed according to the law $N(\mathbf{0}, S_1)$. In this case the McCann's interpolant is known explicitly and in particular, the geodesic curve connecting μ_0 and μ_1 takes the form $\gamma(t) = \{[(1-t)I + t\Lambda]_{\#} \mu\}_t$ with Λ as defined above. Moreover, [22] showed that each point on this geodesic curve is also a Gaussian measure and in fact, for any fixed $t \in [0, 1]$, the probability measure $\gamma(t)$ is characterized by the location parameter $m(t) := (1-t)m_0 + tm_1$ and the dispersion matrix $S(t) := ((1-t)I + t\Lambda)S_0((1-t)I + t\Lambda)$.

Following the above explicit results, the proposed clustering procedure in the case of Gaussian measures can be done in semi-closed form. The related algorithmic procedure is described in Algorithm 2.

Algorithm 2: Wasserstein K-Means (Gaussian Case)

- 1 Choose K measures out of the original observations as the initial cluster centers, $\bar{\mu}_k$, $k = 1, 2, \dots, K$.
- 2 Assign each of the measures μ_i , $i = 1, 2, \dots, n$, to one of the K clusters, selecting the cluster membership $k(i)$ according to the rule

$$k(i) = \arg \min_{k \in \{1, 2, \dots, K\}} \left\{ \|m_i - \bar{m}_k\|_2^2 + Tr \left(S_i + \bar{S}_k - 2(S_i^{1/2} \bar{S}_k S_i^{1/2})^{1/2} \right) \right\}.$$

- 3 Update the cluster centers by estimating the local barycenters using the new members of each cluster by applying the formulas (8)-(9).
- 4 Repeat steps 2-3 until the cluster centers do not change significantly.

2.5 A similarity index and clustering criteria relying on the geodesic curves

In order to offer an alternative and more appropriate proposal to the existing clustering criteria, we construct an index which exploits the geodesic information revealed during the clustering procedure. From the registration problem (6) we are looking to employ the geometric information extracted by this task in order to provide a valid compactness (homogeneity) assessment of the estimated clusters by the Wasserstein K-Means algorithm discussed in 2.2. In particular, consider that K clusters have been derived by Algorithm 1 (or 2) where each one contains n_k probability measures where $n = \sum_{k=1}^K n_k$. For each measure which has been assigned to the k -th cluster (let us denote them as $\mu_{k,i}$ for $k = 1, 2, \dots, K$ and $i = 1, 2, \dots, n_k$), from the related registration procedure, there have been computed the pairs $(\tau_{k,i}, \tilde{\sigma}_{k,i})$. In order to construct a reasonable similarity index we have first to condense the information provided by these pairs to one scalar for each measure. Below we describe the approach we follow.

Assume that n_k probability measures have been assigned to the k -th cluster with cluster center the probability measure $\bar{\mu}_k$ and the parameter triples $\{(\tau_i, \sigma_i, \tilde{\sigma}_i)\}_i$ have been computed for each $i = 1, 2, \dots, n_k$. First, we need to characterize the element (measure) which is closest to the cluster's center, i.e. we define $i_* := \arg \min_{i=1, 2, \dots, n_k} W_2(\mu, \bar{\mu}_k)$ and set $\mu_* = \mu_{i_*}$, $\sigma_* := \sigma_{i_*}$ and $\tilde{\sigma}_* := \tilde{\sigma}_{i_*}$. In this manner, μ_* is set as a the minimal element among the assigned measures in the k -th cluster in the sense that deviates less from the cluster's estimated mean behaviour $\bar{\mu}_k$. Therefore, this element could be used in order to derive some comparison standards in order to better understand the characteristics of the other measures assigned to this cluster. The approach we follow in this attempt is through the comparison and estimation of less distant points (measures) between two geodesic curves. According to that we use the projection of each measure μ_i , i.e. $\gamma_k(\tau_i)$, and we calculate its projection to the geodesic curve that connects the minimal element μ_* and the original measure μ_i . Through this task we cross-validate the result we obtained by the initial registration task described in 2.3.

In particular, for each μ_i assigned in cluster k we define the geodesic curve $\gamma_{i,*}(s)$ connecting the measures μ_* and μ_i with $\gamma_{i,*}(0) = \mu_*$ and $\gamma_{i,*}(1) = \mu_i$. Then, we solve the reverse-registration problem

$$(10) \quad \min_{s \in [0, 1]} W_2(\gamma_{i,*}(s), \gamma_k(\tau_i))$$

which provides the point on the geodesic curve $\gamma_{i,*}(\cdot)$ that deviates less from the point $\gamma_k(\tau_i)$ and parameterized by $s_i \in [0, 1]$ which is considered as the minimizer of problem 10 for i . The rationale between this second projection step is that if the initial measure μ_i is quite similar with the cluster center $\bar{\mu}_k$ then at the second projection we should get a point close to μ_* i.e. $s_i \rightarrow 1$. That means that the double registration procedure will reveal if the measure μ_i really belongs to the interior of the k -th cluster. Observe that if $\mu_i = \mu_*$ then $\gamma_{i,*}(\cdot)$ is simplified to μ_*

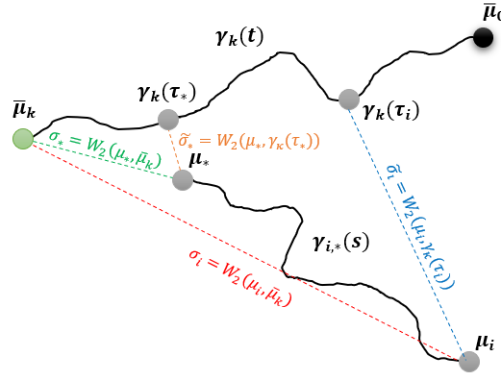


Figure 2: Representation of the geodesic curves involved in the double registration problem.

and the above registration problem is simplified to the reverse projection of $\gamma_k(\tau_*)$ to the initial measure μ_* . For $\mu_i \neq \mu_*$ the interpretation of the minimizers is of particular interest. Let us examine the extreme cases. If $s_i = 0$ and $\tau_i = 0$ then measure μ_i can be characterized as an outlier (observation on the boundary of the cluster). The case where $s_i = 0$ and $\tau_i = 1$ cannot happen since if the initial projection is exactly on $\bar{\mu}_k$ then the solution to the reverse registration problem has only one solution on $s_i = 1$, i.e. μ_* . The case $s_i = 1$ given that $\tau_i = 0$ does not belong to the feasible area of the problem unless if $\bar{\mu}_k = \bar{\mu}_0$. The case $s_i = 1$ given that $\tau_i = 1$ is probably the more “difficult” case since either the measure μ_i coincides with the minimal element or the measure μ_i belongs to the internal area of the cluster or μ_i is an outlier which characteristics deviates more from $\bar{\mu}_0$ than $\bar{\mu}_k$. It is evident that the information obtained from the minimizing pairs (τ_i, s_i) of the double registration problem (optimization problems 6 and 10) is not enough for the full characterization of the status of each point assigned in k -th cluster. Therefore we need to further enhance our distinction argument using the information provided by the distances σ_i and $\tilde{\sigma}_i$ in order to provide a valid measure of homogeneity/compactness of the clusters. The above discussion justifies the definition of the following similarity index.

For each μ_i the *geodesic similarity index* of the k -th cluster center is defined as

$$(11) \quad \tilde{\tau}_{k,i} := \frac{s_i \tau_i \tilde{\sigma}_*}{\tau_* \tilde{\sigma}_i}$$

where (s_i, τ_i) denotes the solution to the double registration problem 6-10 for μ_i . This index is a rescaled version of the initial τ_i , however taking into account also the effect of the true distance from the geodesic curve normalized with respect to the closest point to the cluster center. Clearly, for $\mu_i = \mu_*$ we obtain an index value equal to 1 since it is considered as the ideal case. In particular, due to its convenient scaling, each registration parameter $\tilde{\tau}_{k,i}$ can be realized as the level of certainty/ambiguity regarding the true membership of a particular observation $(\mu_{k,i})$ to the k -th cluster. Clearly, if $\tilde{\tau}_{k,i} \rightarrow 1$ there is a great amount of certainty that the k -th cluster is a very appropriate match for this observation, while if $\tilde{\tau}_{k,i} \rightarrow 0$ there is a great level of ambiguity that the k -th cluster is the most suitable choice for it. Note that, for the clusters that have been derived up to the time the registration parameters are computed, there is no doubt that the assigned observations to these clusters are rightly assigned there. However, small $\tilde{\tau}$ values by many observations indicate a cluster of low homogeneity (non-compact) which maybe reveals a poor initial decision for the number of clusters.

Given that K different clusters have been determined and taking into account all the measures assigned to each cluster, we define the *Geodesic Compactness Index* (GCI) for each one of

the clusters in the following manner

$$(12) \quad GCI_k(K) := \frac{1}{n_k} \sum_{i=1}^{n_k} \tilde{\tau}_{k,i} \text{ for all } k = 1, 2, \dots, K.$$

Moreover, a total compactness index for the total clustering procedure is naturally defined through the weighted sum

$$(13) \quad GCI(K) := \sum_{k=1}^K \frac{n_k}{n} GCI_k(K) = \frac{1}{n} \sum_{k=1}^K \sum_{i=1}^{n_k} \tilde{\tau}_{k,i}.$$

The interpretation of the above indices is in complete accordance with the mean tendency of the similarity indices. A value of the cluster index close to 1 is interpreted as an artifact of high homogeneity of the specific cluster while a an index value close to 0 is interpreted as very low homogeneity of the cluster. Observing low values to the majority of clusters determined indicates that the choice have been made for the number of clusters is maybe not appropriate. On the other hand, observing high values of the compactness indices for the majority of the determined clusters, indicates an appropriate choice for the number of clusters and success in the determination of compact clusters. However, note that if $K = n$ we get that $GCI_1(n) = GCI_2(n) = \dots = GCI_n(n) = 1$ which is clearly not an indication of a good choice for the number clusters but rather a limit case.

3 Applications

3.1 Clustering EU Bond Yields

As a first application we consider the task of clustering the countries of eurozone according to their credit profiles for the time period 2001-2019. The data under consideration is the monthly yield rates for each country's zero coupon government bonds with maturity horizons from one to ten years. The data are collected, on a monthly basis, through the official DataStream database and the countries for which the clustering task is performed are those which were members of the European monetary union constantly for the time period 2001 to 2019. Note that data for Luxemburg are not available (possibly not such type of bonds have been published from its government) therefore it is excluded from the analysis. As a result, the countries included in the analysis (followed by their abbreviations) are: Austria (AT), Belgium (BL), Finland (FI), France (FR), Germany (DE), Greece (GR), Ireland (IE), Italy (IT), Netherlands (NL), Portugal (PT) and Spain (ES).

3.1.1 Credit Profile Determination through Probability Measures

The available data used for the clustering task are for each particular country included in the study, the observed bond indices for each different maturity horizon as it is recorded at the end of each month. For example, for a two year period, for the country i there are available 24 records for the published by the country's government bonds with maturity horizon $m = 1, 2, \dots, 10$ years. Therefore, a record at the specified time t (i.e. at the end of a certain month in the time period under consideration) is the vector

$$\mathbf{r}_t^{(i)} = \left(r_{t,1}^{(i)}, r_{t,2}^{(i)}, \dots, r_{t,10}^{(i)} \right)' \in \mathbb{R}^{10}$$

where each $r_{t,m}^{(i)}$ for $m = 1, 2, \dots, 10$ denotes the recorded index for the bond with maturity horizon m years. As a result, if the period under consideration consists of n months, then for each country there is available a $(n \times 10)$ data matrix with the available records.

Given that the economies are in a steady state, no major variations in these records should be observed in each month. For this reason, the entire time period 2001-19, that data are available, is split into six smaller in periods: 2001-04, 2005-08, 2009-11, 2012-14, 2015-17 and 2018-19 in order to not allow very lengthy time periods where important changes may occur and significantly affect each country's economy. These periods represent a growth period (2001-04), followed by two financial crisis intervals: 2005-08, which is the period up to the Lehman brothers collapse, and 2009-11 that is the immediate aftermath, including the ensuing debt crisis in Greece, Portugal and Ireland. These are followed by a period when certain eurozone countries were under Economic Adjustment programmes (bailout programmes, 2012-14), a period following these programmes (2015-17) and the last two recovery years (2018-19). It is evident that one may try different time intervals (6 months, 1 year periods, etc.) or use more frequent data (e.g. daily, weekly, etc.) however since this is not the main purpose of this paper we attempt to keep such details to the most convenient for the analysis and the reader framework.

Clearly, the provided data in the current form is quite hard to analyze. Therefore, we attempt for each one of the defined time periods, to condense the available data for each country in order to sufficiently and more conveniently represent the provided information. That task is performed through the identification of each data matrix by a probability measure of the Location-Scatter family of distributions, for convenience we restrict ourselves to the family of Gaussian measures. Under this approach, for a certain data matrix (i.e. provided data for a specific country i) the location vector $\mathbf{m}_i \in \mathbb{R}^{10}$ represents the mean tendency of the bond indices for the particular period of time therefore it is reasonable to set

$$\mathbf{m}_i = \bar{\mathbf{r}}_i = (\bar{r}_{i,1}, \bar{r}_{i,2}, \dots, \bar{r}_{i,10})' \in \mathbb{R}^{10}$$

where $\bar{r}_{i,m} = \mathbb{E}[r_{t,m}^{(i)}] \in \mathbb{R}$ for $m = 1, 2, \dots, 10$ denoting the mean tendency of the bond index of maturity horizon m for the country i . Another important characteristic of the dataset is the correlation structure between the bonds of different maturity and of course their dispersion. Under the assumption that the nature of the data does not change significantly during our sample period, then the dispersion characteristics can be sufficiently estimated by the covariance matrix

$$S_i = \mathbb{E}[(\mathbf{r}_t^{(i)} - \bar{\mathbf{r}}_i)(\mathbf{r}_t^{(i)} - \bar{\mathbf{r}}_i)'] \in \mathbb{R}_+^{10 \times 10}.$$

Under this setting, the country's i profile can be identified with the Gaussian probability measure $\mu_i = N(\mathbf{m}_i, S_i)$ by condensing the information provided by the data set to location and dispersion-correlation characteristics. This is a very natural approach in most applications considering multivariate data however, one may consider also some family of probability distributions capturing asymmetries in data (e.g. through a Copula, a meta-distribution, a vine-Copula construction, etc.). However, since in this work we investigate the case of the Location-Scatter family of distributions we feel that such a consideration, although extremely interesting, it is beyond the scope of this paper. Therefore, under the above considerations, the credit profile of a country induced by the observed bond yield data can be represented by a Gaussian measure where the location and dispersion parameters efficiently condense the available information provided for the time period under consideration and the nature of the Gaussian law reflects the assumption regarding consistency, i.e. the time period length is chosen so that no dramatic changes happen in the economies of the countries under study for its duration.

3.1.2 Clustering bond yield data with Wasserstein barycenters

Following the aforementioned framework and the learning methodology described in Section 2.2, we perform the clustering analysis of the credit profiles of the eurozone countries. The clustering task is performed repeatedly for the defined six time periods 2001-04, 2004-08, 2009-11, 2012-14, 2015-17 and 2018-19. First, we employ the geodesic criterion presented in Section 2.5 in order to determine a reasonable number of clusters for each time period. The results of

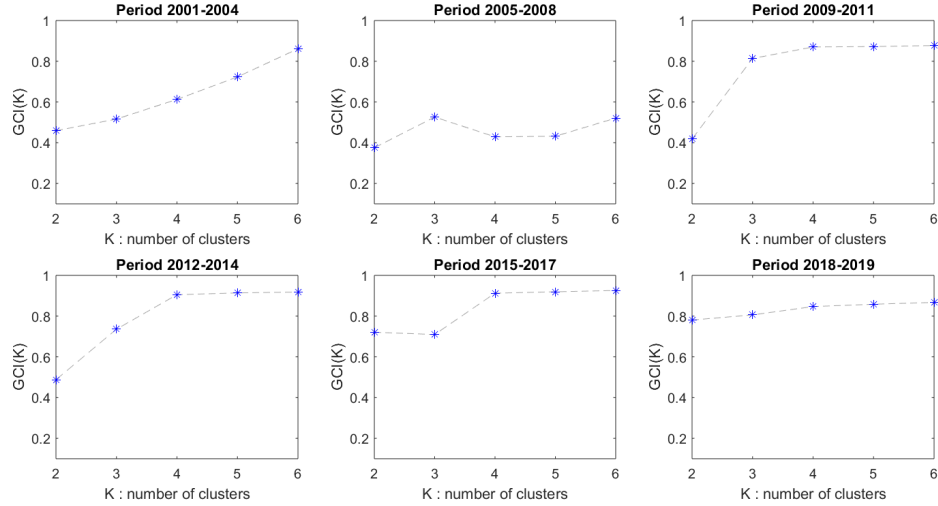


Figure 3: Geodesic Compactness Index values per time period

the criterion output are graphically represented in Figure 3. We consider up to six different clusters for each time period, since more clusters may not have any interpretative value. The rationale beyond the selection of an appropriate number of clusters in each case, is to choose the number of groups where a high value (comparing to the values for other group numbers) in the compactness is succeeded and adding more groups this number is not significantly increased. Having this in mind, the optimal cluster numbers per time period are: 4 for 2001-04, 3 for 2005-08, 4 for 2009-11, 4 for 2012-14, 4 for 2015-17 and 3 for 2018-19.

Time Period	2001-04	2005-08	2009-11	2012-14	2015-17	2018-19
Group 1	DE	AT BL DE FI FR NL	AT BL DE FI FR NL	AT BL DE FI FR NL	AT BL DE FI FR IE NL	AT BL DE FI FR IE NL
Group 2	AT	GR IT	ES IT	ES IE IT	ES IT	ES PT
Group 3	BL ES FI FR NL	IE	IE PT	PT	PT	GR IT
Group 4	GR IE IT PT		GR	GR	GR	

Table 1: Optimal clusters according to GCI interpretation

It seems that for the period 2001-2008 for most choices of clusters' number, the compactness index is not higher than 0.65 (higher index value are obtained for the period 2001-04 for $K > 4$ however this happens because creates clusters of a single country) indicating not very high homogeneity in the clustering output. On the other hand, the clustering outputs in the period 2009-2019 is characterized by quite high homogeneity with the majority of cases (for $K > 2$) succeeding a compactness index close to or above 0.8. For each time period, the obtained clusters are illustrated in Table 1 and the compactness index of each cluster in Table 2.

	2001-04	2005-08	2009-11	2012-14	2015-17	2018-19
Group 1	1.00	0.41	0.94	0.95	0.92	0.90
Group 2	1.00	0.75	0.82	0.76	0.79	0.51
Group 3	0.58	1.00	0.64	1.00	1.00	0.78
Group 4	0.46	-	1.00	1.00	1.00	-
Total	0.61	0.53	0.81	0.90	0.91	0.81

Table 2: GCI values per time period and cluster

	AT	BL	DE	ES	FI	FR	GR	IE	IT	NL	PT
2001	AAA	AA+	AAA	AA+	AA+	AAA	A	AAA	AA	AAA	AA
2002	AAA	AA+	AAA	AA+	AAA	AAA	A	AAA	AA	AAA	AA
2003	AAA	AA+	AAA	AA+	AAA	AAA	A+	AAA	AA	AAA	AA
2004	AAA	AA+	AAA	AAA	AAA	AAA	A	AAA	AA-	AAA	AA
2005	AAA	AA+	AAA	AAA	AAA	AAA	A	AAA	AA-	AAA	AA-
2006	AAA	AA+	AAA	AAA	AAA	AAA	A	AAA	A+	AAA	AA-
2007	AAA	AA+	AAA	AAA	AAA	AAA	A	AAA	A+	AAA	AA-
2008	AAA	AA+	AAA	AAA	AAA	AAA	A	AAA	A+	AAA	AA-
2009	AAA	AA+	AAA	AA+	AAA	AAA	BBB+	AA	A+	AAA	A+
2010	AAA	AA+	AAA	AA	AAA	AAA	BB+	A	A+	AAA	A-
2011	AAA	AA	AAA	AA-	AAA	AAA	CC	BBB+	A	AAA	BBB-
2012	AA+	AA	AAA	BBB-	AAA	AA+	B-	BBB+	BBB+	AAA	BB
2013	AA+	AA	AAA	BBB-	AAA	AA	B-	BBB+	BBB	AA+	BB
2014	AA+	AA	AAA	BBB	AA+	AA	B	A	BBB-	AA+	BB
2015	AA+	AA	AAA	BBB+	AA+	AA	CCC+	A+	BBB-	AAA	BB+
2016	AA+	AA	AAA	BBB+	AA+	AA	B-	A+	BBB	AAA	BB+
2017	AA+	AA	AAA	BBB+	AA+	AA	B-	A+	BBB	AAA	BBB-
2018	AA+	AA	AAA	A-	AA+	AA	B+	A+	BBB	AAA	BBB-
2019	AA+	AA	AAA	A	AA+	AA	BB-	A+	BBB	AAA	BBB

Figure 4: S&P yearly credit ratings for the EU countries for the time period 2001-2019

From early on (2001-04), our proposed framework and methodology appears able to identify a cluster of the so-called PIIG countries (Portugal, Ireland, Italy and Greece), whose bond yields indicated back then that a debt crisis might ensue. During the eurozone debt crisis (2009-11) and the resulting bailout programmes (2012-14) Greece, the country with the most acute debt problem, is singled out as a different cluster, while Ireland and Portugal (countries under bailout programs) are grouped into a separate cluster. After the end of the bailout programs in all countries (2018-19), Ireland has “moved” to the core eurozone Group 1, Greece and Italy remain the countries with the highest debt-to-GDP in the eurozone (Group 3), while the Iberia countries (Spain and Portugal) constitute a separate cluster in-between. In order to assess the validity of the obtained clustering outputs, in Figure 4 are illustrated the credit rankings of each eurozone country for the period 2001-19 on a yearly base as determined by Standard and Poor (S&P). It is evident, that the clustering approach we followed succeeded in retrieving the true situation in most of the cases if we consider the rating mechanism of S&P as an expert opinion.

3.2 Image classification with Wasserstein barycenters in remote sensing

In this section, we employ the learning methodology described in Section 2 in a standard problem in remote sensing, that of characterizing satellite images, i.e. assigning the pixels of satellite images to certain category types, e.g. built environment, agricultural environment, etc. The general practice in this task is to use as trainset for each category some sampled pixels from previous classification tasks in order to train the classification mechanism, and then use the trained system to characterize the areas of the new image. In the following, we first describe the proposed framework and then the new classification methodology is implemented for the full characterization of a satellite image taken from the area of Mesogeia, Attica, Greece (Figure 5).

3.2.1 Description of the framework

Assume that an image is available in resolution $r \times c$, i.e. it consists of $M := r \times c$ pixels. Then each pixel p_i for $i = 1, 2, \dots, M$ is identified by a specific pair of coordinates (x_i, y_i) that describe the pixel’s position in the image and by a specific vector $p_i \in \mathbb{R}^d$ representing the



Figure 5: The satellite image from the Mesogeaia area

pixel's brightness on each color band according the color band system is used, e.g. if the RGB color band system is used, then $d = 3$ and $p_i \in \mathbb{R}^3$ for all i . At the time when the satellite image is taken, each pixel belongs to a specific environment type (e.g. built environment, agricultural, green areas, etc), however this category is not a priori known but it must be inferred from the available information, i.e. the values in the different color bands of the pixel and from what lies in its neighbourhood. In order to determine the environment type of each pixel, statistical methods are employed relying on databanks with classified pixels in order to characterize the new image. Below, following the discussion in Section 2 regarding the clustering/classification capabilities of probability (Wasserstein) barycenters, a learning approach is presented relying on a distributional-wise framework of the data unlike other statistical methods relying on local criteria like least-squares or the maximum likelihood principle .

Assume that a train set of M pixels of K different environment types is available in order to properly prepare a classification scheme for the identification of the unknown areas of a satellite image. Denote by $\{p_i^k\}_{i=1}^{M_k}$ the classified sample belonging to the k -th environment type, where $M = \sum_{k=1}^K M_k$. Then, for each pixel p_i^k , $i = 1, 2, \dots, M_k$ of any category $k = 1, 2, \dots, K$, we define a neighborhood around it (for a given radius) and define the parameters

$$m_i^k := p_i^k \in \mathbb{R}^d,$$

describing the *location* of the pixel in the color band system that is used, and

$$S_i^k := \frac{1}{M_k^{(i)}} \sum_{j=1}^{M_k^{(i)}} (p_j^k - m_i^k)(p_j^k - m_i^k)^T \in \mathbb{R}_+^{d \times d},$$

describing the *dispersion* in color band values in the pixel's neighborhood where $M_k^{(i)}$ is the number of the pixels in the neighborhood of p_i^k . Naturally, each pixel p_i^k can be identified by a probability measure of the Location-Scatter family, $\mu_i^k = LS(m_i^k, S_i^k)$ (e.g. a Gaussian probability measure on \mathbb{R}^d). Realising each pixel as a probability measure with the above manner, besides the information regarding the location of the specific point, are also parameterized the characteristics of its neighbourhood around it through the dispersion matrix S_i^k . Quantifying the information in the neighbourhood of the pixel through the covariance matrix treats also the problem of different orientation. Consider for example two pixels of the same type with exactly the same neighbourhood but rotated. Under the scope of a covariance matrix these neighbourhoods are exactly the same while in other approaches this is not true.

In the case of Gaussian probability laws, the pixels of the k -th environment type, are identified by an appropriately assigned collection of Gaussian probability measures $\mathcal{M}_k = \{\mu_i^k\}_{i=1}^{M_k}$.

Since, all these probability measures parameterize location and dispersion characteristics of pixels belonging to the same category, we need to characterize this category’s most typical element. Under the probabilistic framework we work, we employ the concept of Wasserstein barycenter in order to define the mean tendency of a pixel that should be assigned to this particular category. Then, for each environment type k , the corresponding probability barycenters are estimated in order to obtain a prototype for each environment, i.e. for each category k , the barycentric probability measure is

$$\bar{\mu}_k = \arg \min_{\mu \in \mathcal{P}} \frac{1}{M_k} \sum_{i=1}^{M_k} \mathcal{W}_2^2(\mu, \mu_i^k)$$

where $\bar{\mu}_k \in \mathcal{P}(\mathbb{R}^d)$ remains a probability measure of the Location-Scatter family where its parameters can be calculated semi-analytically (see Section 2.4).

Following the above procedure, the training dataset (i.e. the classified samples) provides K characteristic barycenters and this summarized information can be used in order to characterize any unclassified image according to these K specified environment types. In this case, the above procedure is repeated in order to identify each pixel p_j in the uncharacterized image by a probability measure $\mu_j \in LS$ (working as above with the pixels in its neighbourhood). Then, these pixels are classified to a specific environment type according to the rule

$$k(j) := \arg \min_{k \in \{1, 2, \dots, K\}} \mathcal{W}_2^2(\mu_j, \bar{\mu}_k).$$

Therefore, each unclassified pixel p_j is classified to the environment type k that the specific pixel’s identified measure deviates less from the category’s corresponding barycenter.

Remark 3.1. At this point we would like to emphasize on the difference of the proposed learning approach with other methods used in remote sensing literature. Approaches which seems close to the discussed one are learning methods (classification or clustering) which rely on the Mahalanobis distance (see e.g. [5, 12, 30]). Clearly, Mahalanobis distance provides a distance between a point (vector) and the induced probability distribution from a sample if can be identified by a member of the Location-Scatter family. Although taking into account distributional characteristics from the sample, this approach is still a point-wise one since no distributional characteristics regarding the point (pixel’s neighbourhood) are considered. On the other hand, the discussed method employing the Wasserstein distance and treating each point as a probability distribution takes into account distributional characteristics of both samples and observations. In remote sensing this aspect is of particular importance, since by this mean is introduced in the analysis information regarding the neighbourhood of each pixel and each pixel is considered as a puzzle piece instead of just a point. Consider for example two pixels p_A and p_B where the first one has on its north neighbourhood sea and urban structure anywhere else, while the second one has sea on its east neighbourhood and urban structure anywhere else. Under the Wasserstein distance both pixels are classified in the same category regardless the different orientation of its neighbourhood (no permutations needed). In advance to the Mahalanobis distance, this metric sense uses also dispersion characteristics of the pixel with respect to the area around it instead of using only the pixel’s brightness.

3.2.2 A case study

As a practical illustration of the described methodology we characterize a satellite image taken from the area of Mesogeia, Attica, Greece (Figure 5). The colour band system used is a 6-band system, i.e. $p_i \in \mathbb{R}^6$. For simplicity, only four environment types are used and specifically: 1 - built environment (red), 2 - agriculture (yellow), 3 - green areas (green) and 4 - sea (blue). As a training dataset are used four samples, one for each environment type of corresponding sizes $n_1 = 294$, $n_2 = 1214$, $n_3 = 611$ and $n_4 = 105$. Using these samples as a training

base we characterize the unclassified image using the approach described in Section 3.2.1. The classification accuracy is confirmed through $N = 3031$ pixels of known classification (176 of urban type, 1842 of agricultural type, 159 from sea and 854 of green areas). For this first task, different neighbourhood sizes are used for the derivation of location and dispersion parameters for each pixel. In particular neighbourhood sizes of 8 pixels (8-p), 24 pixels (24-p), 48 pixels (48-p), 96 pixels (96-p), 192 pixels (192-p) and 4096 pixels (4096-p) are considered. The classification results (please see Table 3) indicate that the chosen neighbourhood size do not affect that much the classification task, at least in the case where each environment type is represented through a single barycenter. In general, with that choice (single barycenters) a total accuracy around 83% is succeeded for all neighbourhood sizes under consideration. However, it is evident that in some categories like Agriculture and Green Areas the individual accuracy is not very high which could be the effect of low representative power of the specific categories through the use of single barycenters.

Neighbourhood size	Accuracy per Environment Type				Total Accuracy
	Built Env.	Agriculture	Green Areas	Sea	
8-p	81.25%	77.56%	71.43%	100.00%	82.56%
24-p	82.39%	78.64%	71.25%	100.00%	83.07%
48-p	81.82%	78.50%	71.43%	100.00%	82.94%
96-p	81.82%	78.53%	71.10%	100.00%	82.86%
192-p	82.29%	78.72%	70.96%	100.00%	82.99%
4096-p	82.56%	78.98%	69.77%	100.00%	82.83%

Table 3: Classification results using single barycenters for different neighbourhood sizes

As a next step in our analysis we employ more barycenters for each category in order to increase the representability of the category’s variability through more factors (local barycenters). For example, it seems that the information of the agricultural environment is not quantified efficiently through the use of a single barycenter. For this reason, the use of more barycenters for the representation/characterization of the same category could enhance the classification performance of the method since different fragments of information are expected to be captured by different local barycenters. Therefore, before the classification task, a local clustering step for each one of the environment types should reveal better options for the representation of each category (through more barycenters). This is a quite rational approach since the different categories present different homogeneity, e.g. sea environment is more homogeneous since a pixel of this category in its neighbourhood could possibly have either sea or coast (i.e. built environment) therefore maybe two clusters could properly model this distinction. On the other hand, environment types like agricultural should need more than one clusters (and consequently more barycenters) to properly describe the provided information since present high levels of heterogeneity due to the variety of their possible neighbours, e.g. a farm pixel could be neighbour with urban, forest or sea environment or with any combination of them. As a result, the use of more clusters (barycenters) for the description of more heterogenous environment types seems a very justified approach.

However, there is a question on how to optimally select an appropriate number of clusters (i.e. barycenters) for each environment type. Although, the derivation of a universal optimal criterion is not possible since different types of data should need different treatment, the compactness criterion discussed in Section 2.5 could offer a very convenient and plausible mean of discrimination. This compactness index can be used to provide an intuition for the minimum number of clusters that are needed in order to model the information of each environment type by creating homogeneous (compact) clusters. In Figure 6 are illustrated plots for the value of index $GCI(K)$ for different choices of clusters (for $K_j = 1, 2, \dots, 10$) for each environment type $j = 1, 2, 3, 4$. It seems that for the built environment type at least two barycenters should be

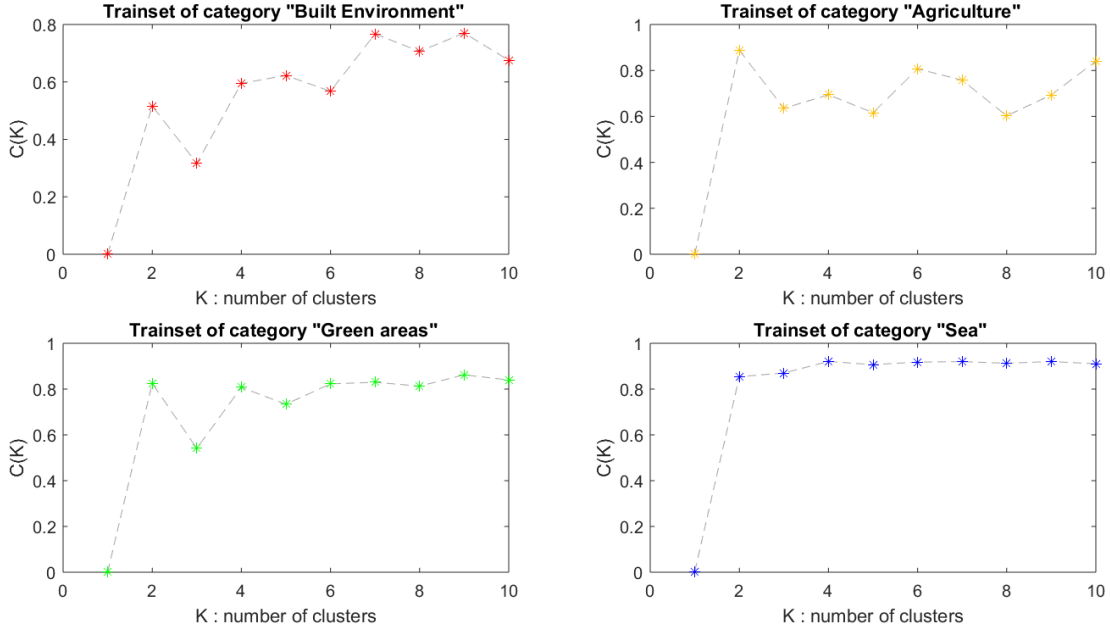


Figure 6: Geodesic Compactness Index values per environment type

used while the same number of barycenters looks sufficient also for the sea category. Also, for the other two categories (agricultural environment and green areas) it seems that the minimum number of barycenters that should be used is at least two, however the use of more than two barycenters is also a very natural choice. Therefore, the occurring classification scheme should represent each environment type with more than one centroids (barycenters) which although different lead to the same classification result if an uncharacterized area is closer to just one of these centroids with respect to centroids from other environment types. For example, if on the training task, each environment type j (for $j = 1, 2, 3, 4$) is divided into $K_j > 1$ sub-categories, then the final classification scheme should consist of $K = \sum_{j=1}^4 K_j > 4$ categories, however the final category assignment concerns only the initial 4 environment types.

Barycenters Model	Accuracy per Environment Type				Total Accuracy
	Built Env.	Agriculture	Green Areas	Sea	
$K_{1111} = 4$	81.82%	78.50%	71.43%	100.00%	82.94%
$K_{2222} = 8$	83.52%	80.35%	87.59%	100.00%	87.87%
$K_{3333} = 12$	91.48%	79.97%	77.87%	100.00%	87.33%
$K_{4444} = 16$	90.91%	82.79%	89.70%	100.00%	90.85%
$K_{5555} = 20$	89.77%	78.07%	87.47%	100.00%	88.83%
$K_{6666} = 24$	90.34%	86.32%	85.83%	100.00%	90.62%
$K_{7777} = 28$	88.64%	86.05%	87.35%	100.00%	90.51%
$K_{8888} = 32$	92.05%	83.98%	92.39%	100.00%	92.11%
$K_{3582} = 17$	86.93%	82.25%	94.61%	100.00%	90.95%
$K_{4781} = 20$	88.64%	85.07%	93.09%	99.37%	91.54%
$K_{4782} = 21$	88.64%	85.07%	92.97%	100.00%	91.67%

Table 4: Classification results using multiple barycenters models for 48-p neighbourhood size

In general, a good choice for the number of sub-clusters in categories that present high heterogeneity should balance between accuracy improvement and the possible effect of over-parameterization. In Table 4 is illustrated the accuracy of the classification procedure for

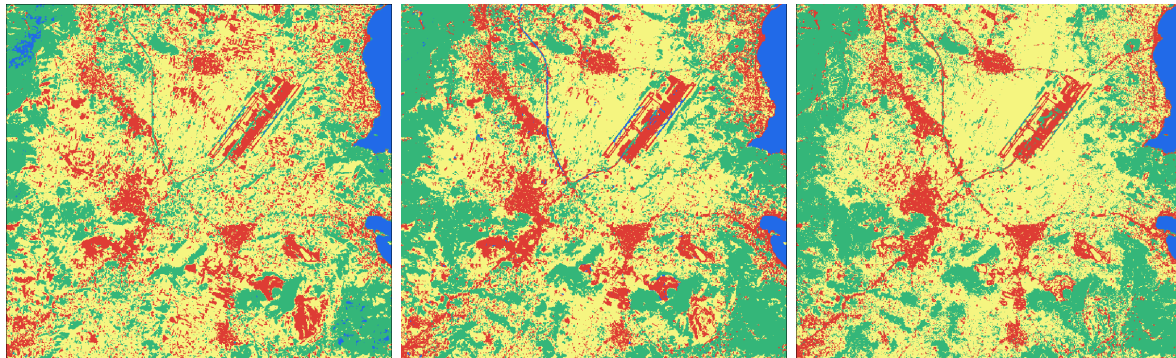


Figure 7: Image characterization using (a) single barycenters (left) (82.94%), (b) two local barycenters for each environment type (middle) (87.87%) and (c) multiple barycenters most efficient model (right) (91.54%)

different choices of sub-clusters. Clearly, an improvement of about 10% in total accuracy is succeeded comparing to the accuracy succeeded with single barycenters, justifying the further information allocation to more local centroids.

4 Conclusions

In this work we presented a learning approach for measure-valued data relying on the concept of Wasserstein barycenter. In particular, we focus on the case of the Location-Scatter family of probability measures where a clustering procedure based on the K-means algorithm is proposed, accompanied by a criterion for the optimal selection of the number of clusters relying on geometric arguments of the underlying space of probability measures that we work. The proposed learning approach can be used either as a supervised or as an unsupervised learning scheme with substantial success, and this fact is illustrated on the applications in clustering credit profiles and remote sensing considered in this paper. The proposed learning approach seems reasonable when data under consideration evolve in time like bond data considered in the first application in the paper where the proposed clustering approach seems that reveals the true situation. Moreover, several capabilities of probability barycenters exploited during the implementation of the discussed learning approach in remote sensing where both clustering and classification tasks combined with very good results.

Acknowledgements

Georgios N. Domazakis kindly thanks Erwin Schrödinger International Institute for Mathematics and Physics for financial support and hospitality in Vienna, Austria, during the thematic programme on “Optimal Transport” in May 2019.

References

- Aggarwal, C. C. (2010). *Managing and mining uncertain data* (Vol. 35). Springer Science & Business Media.
- Aggarwal, C. C., Hinneburg, A., & Keim, D. A. (2001). On the surprising behavior of distance metrics in high dimensional space. In *International conference on database theory* (pp. 420–434).

- Agueh, M., & Carlier, G. (2011). Barycenters in the Wasserstein space. *SIAM Journal on Mathematical Analysis*, 43(2), 904–924.
- Alvarez-Esteban, P. C., del Barrio, E., Cuesta-Albertos, J., & Matrán, C. (2016). A fixed-point approach to barycenters in Wasserstein space. *Journal of Mathematical Analysis and Applications*, 441(2), 744–762.
- Atkinson, P. M., & Lewis, P. (2000). Geostatistical classification for remote sensing: an introduction. *Computers & Geosciences*, 26(4), 361–371.
- Bhatia, R., Jain, T., & Lim, Y. (2019). On the Bures–Wasserstein distance between positive definite matrices. *Expositiones Mathematicae*, 37(2), 165–191.
- Bouveyron, C., Girard, S., & Schmid, C. (2007). High-dimensional data clustering. *Computational Statistics & Data Analysis*, 52(1), 502–519.
- Chiou, J.-M., & Li, P.-L. (2007). Functional clustering and identifying substructures of longitudinal data. *Journal of the Royal Statistical Society: Series B (Statistical Methodology)*, 69(4), 679–699.
- De Amorim, R. C., & Mirkin, B. (2012). Minkowski metric, feature weighting and anomalous cluster initializing in K-means clustering. *Pattern Recognition*, 45(3), 1061–1075.
- de Carvalho, F. d. A., Brito, P., & Bock, H.-H. (2006). Dynamic clustering for interval data based on l_2 distance. *Computational Statistics*, 21(2), 231–250.
- De Carvalho, F. d. A., & Lechevallier, Y. (2009). Partitional clustering algorithms for symbolic interval data based on single adaptive distances. *Pattern Recognition*, 42(7), 1223–1236.
- Ghosh, A., Mishra, N. S., & Ghosh, S. (2011). Fuzzy clustering algorithms for unsupervised change detection in remote sensing images. *Information Sciences*, 181(4), 699–715.
- Goutte, C., Toft, P., Rostrup, E., Nielsen, F. Å., & Hansen, L. K. (1999). On clustering fMRI time series. *NeuroImage*, 9(3), 298–310.
- Haggarty, R., Miller, C., & Scott, E. (2015). Spatially weighted functional clustering of river network data. *Journal of the Royal Statistical Society: Series C (Applied Statistics)*, 64(3), 491–506.
- Hastie, T., Tibshirani, R., & Friedman, J. (2009). *The elements of statistical learning: data mining, inference, and prediction*. Springer Science & Business Media.
- Irpino, A., & Verde, R. (2008). Dynamic clustering of interval data using a Wasserstein-based distance. *Pattern Recognition Letters*, 29(11), 1648–1658.
- Jacques, J., & Preda, C. (2014). Model-based clustering for multivariate functional data. *Computational Statistics & Data Analysis*, 71, 92–106.
- Kim, Y.-H., & Pass, B. (2017). Wasserstein barycenters over Riemannian manifolds. *Advances in Mathematics*, 307, 640–683.
- Le Gouic, T., & Loubes, J.-M. (2017). Existence and consistency of Wasserstein barycenters. *Probability Theory and Related Fields*, 168(3-4), 901–917.
- Liao, T. W. (2005). Clustering of time series data - A survey. *Pattern recognition*, 38(11), 1857–1874.

- Masarotto, V., Panaretos, V. M., & Zemel, Y. (2019). Procrustes metrics on covariance operators and optimal transportation of Gaussian processes. *Sankhya A*, 81(1), 172–213.
- McCann, R. J. (1997). A convexity principle for interacting gases. *Advances in mathematics*, 128(1), 153–179.
- Monge, G. (1781). Mémoire sur la théorie des déblais et des remblais. *Histoire de l'Académie Royale des Sciences de Paris*.
- Papayiannis, G. I., & Yannacopoulos, A. N. (2018). A learning algorithm for source aggregation. *Mathematical Methods in the Applied Sciences*, 41(3), 1033–1039.
- Ray, S., & Mallick, B. (2006). Functional clustering by Bayesian wavelet methods. *Journal of the Royal Statistical Society: Series B (Statistical Methodology)*, 68(2), 305–332.
- Santambrogio, F. (2015). Optimal transport for applied mathematicians. *Birkhäuser, NY*, 55, 58–63.
- Tuzel, O., Porikli, F. M., & Meer, P. (2007). Human detection via classification on Riemannian manifolds. *2007 IEEE Conference on Computer Vision and Pattern Recognition*, 1-8.
- Vapnik, V. (2013). *The nature of statistical learning theory*. Springer science & business media.
- Villani, C. (2003). *Topics in optimal transportation* (No. 58). American Mathematical Soc.
- Xiang, S., Nie, F., & Zhang, C. (2008). Learning a Mahalanobis distance metric for data clustering and classification. *Pattern recognition*, 41(12), 3600–3612.
- Zemel, Y., Panaretos, V. M., et al. (2019). Fréchet means and Procrustes analysis in Wasserstein space. *Bernoulli*, 25(2), 932–976.